**12** *Egypt. J. Chem.* **58**, No. 2, pp. 217- 235 (2015)

# Corrosion Inhibition of New Prepared Cationic Surfactant on Carbon Steel in Acidic Media

**E.A. Badr and A.I. Adawy**
*Petrochemical Department, Egyptian Petroleum Research Institute, Cairo, Egypt.*

IN this study, three cationic surfactants were prepared by esterfication of different fatty alcohols like dodecyl alc., tetradecyl alc. and hexadecyl alc. with bromoacetic acid then reaction with diphenyl amine then quaternized the resulted tertiary amines with trimethyl phosphate to produce a series of quaternary ammonium salts. FTIR spectra and $H^1$ NMR spectrum were performed to confirm compound structure. Surface tension of these surfactants was measured. The surface and the thermodynamic parameters were calculated.

The corrosion inhibitions of prepared surfactant were studied by weight loss, potentiodynamic polarization and electrochemical impedance spectroscopy (EIS) techniques. The inhibition efficiencies obtained from all techniques are in good agreement with each other. The potentiodynamic polarization measurements indicate that the inhibitors were mixed type.

**Keywords**: Cationic surfactants, Surface parameters, Adsorption and Corrosion**.**

Evaluation of mild steel corrosion phenomena has become important especially in acidic media because acids are the most commonly used type of aggressive solutions or pickling [1.2], cleaning [3], descaling [4] and oil-well acidization [5]. Mineral acids solutions are often used which are also corrosive to steel but these detrimental effects of corrosion caused by the acids can be reduced by the addition of corrosion inhibitors in small concentrations [6-9].

Corrosion inhibitors are used to prevent corrosion and damage that would cause harm during production or use of materials. The most important inhibitors are the adsorption-inhibitors containing hetero atoms such as nitrogen, oxygen, sulphur, and phosphorous atoms [10]. They are adsorbed onto the surface of the metal within an acidic media, thus resulting in an adsorption-film acting as barrier by separating the metal from the corrosive medium and blocking the

active sites. Several techniques such as anodic or cathodic protection, coating layer on the metal, oxidizing or phosphatizing treatment have been used to reduce the corrosion of metal [11,12], some of these techniques are expensive and may require high production cost of the final product. So, the search for the most efficient, nontoxic and cheap inhibitor has been of great interest.

Surfactant molecules have been broadly employed in order to minimize and control metal corrosion, effectively forming interfacial films on metallic surfaces that protect them by impairing the action of electrolytes [13]. The intrinsic ability of surfactant molecules to easily adsorb on surfaces and interfaces is associated with their amphiphilic structure. In solid–liquid systems, they form a protecting interfacial film against the action of corrosion agents [14]. The adsorption of surfactants on metal surfaces depends on the structure and concentration of surfactant molecules in the contacting medium, determining the final adsorption layout with the formation of monolayers or multilayers of surfactant molecules[15].

The cationic surfactant of n-alkyl-quaternary ammonium salts is considered to be the most effective corrosion inhibitor on iron and steel in HCl and $H_2SO_4$ acid [16,17].

The objective of this investigation is to determine the corrosion inhibition efficiency of (Ib, IIb and IIIb) as a novel inhibitor for the corrosion of carbon steel in 1.0 M HCl and to calculate the surface parameters of the synthesized surfactant. The inhibition efficiency was determined using three different techniques: electrochemical impedance spectroscopy (EIS), potentiodynamic polarization and gravimetric measurements.

## Experimental Procedure

*Materials*

The chemicals used in this study were of pure grade from Aldrich and were used without further purification. The solvents used were of pure grade.

*Synthesis*

1 mole of different fatty alcohols; dodecyl alc., tetradecyl alc. and hexadecyl alc., and 1 mole of bromoacetic acid were refluxed in DienShtark system respectively in presence of xylene as a solvent until a definite amount of water removed. The solid product was dried under vacuum to obtain ester compounds I, II and III.

0.5 mole of diphenyl amine and 0.5 mole of ester compounds I, II and III in one neck flask were refluxed respectively for six hours in benzene as a solvent. The reaction mixtures were left to cool then filtered to produce tertiary amines Ia, IIa and IIIa.

*Synthesis of cationic surfactants*

1 mole of trimethyl phosphate and 1 mole of different tertiary amines Ia, IIa and IIIa in one neck flask were refluxed respectively for ninety hours in benzene as a solvent. The solid product was dried under vacuum and recrystallized from benzene to obtain the cationic surfactants alkyl acetate methyldiphenyl ammonium salt Ib, IIb and IIIb.

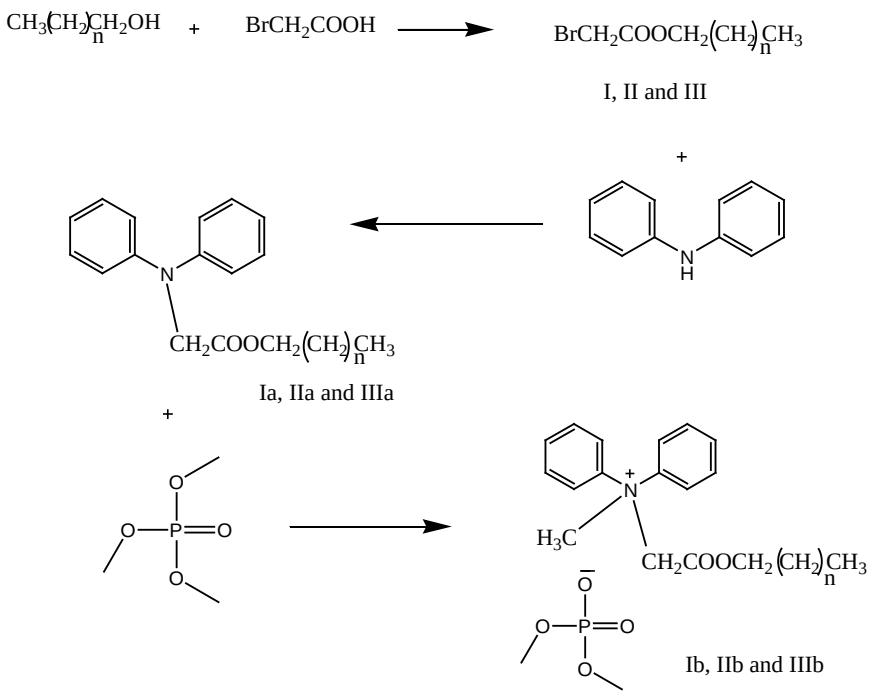


**Scheme 1 . Preparation of different cationic surfactants**
n = 10 (I : Ib), 12 (II : IIb) and 14 (III : IIIb)

*Structural confirmations of the prepared compounds*

The chemical structure of the synthesized compounds was characterized by:

1. FTIR spectra were obtained using ATI Mattsonm Infinity series™, Bench top 961 controlled by Win First™ V2.01 software. (Egyptian Petroleum Research Institute).

2. $^1$HNMR was measured in DMSO-$d_6$ by Spect Varian, GEMINI 200 ($^1$H 200 MHz). (Micro Analytical Center, Cairo University).

*Evaluation method of surface active properties*

*Surface tension*

Surface tension of the prepared compounds solutions were measured using Du-Nouy Tensiometer (Krusstype 6). The surface tension of different

concentrations range of $4x10^{-2}$ to $1.9x10^{-5}$ mole/liter in temperature equal to 20°C was measured.

*Surface parameters of the prepared compounds*

*Critical micelle concentration (CMC):* The values of the critical micelle concentration of the prepared compounds were determined using surface tension techniques. Where in this method, values of the surface tension measurements were plotted against the corresponding concentrations. The interrupt change in the SC curves express on the CMC concentrations.

*Effectiveness ($\pi_{CMC}$):* $\pi_{CMC}$ is the difference between the surface tension of the pure water ($\gamma_o$) and the surface tension of the surfactant solution ($\gamma$) at the critical micelle concentration.

$$\pi_{CMC} = \gamma_o - \gamma_{CMC} \qquad 1$$

*Efficiency ($PC_{20}$)*: Efficiency ($PC_{20}$) is determined by the concentration (mol/liter) of the surfactant solutions able to suppress the surface tension by 20 dyne/cm.

*Maximum surface excess $\Gamma_{max}$:*The values of the maximum surface excess $\Gamma_{max}$ calculated from surface or interfacial data by the use of Gibbs equation[18].

$$\Gamma_{max} = \frac{1}{2.303nRT}\left(\frac{\partial\gamma}{\partial log C}\right) \qquad 2$$

where

$\Gamma_{max}$ maximum surface excess in mole/cm$^2$

n number of solute species and equal to 2 for conventional ionic surfactants

R universal gas constant 8.31 x $10^7$ ergs mole$^{-1}$ K$^{-1}$

T absolute temperature (273.2 + °C)

$\delta\gamma$ surface pressure in dyne/cm

*C surfactant concentration*

($\delta\gamma/\ \delta$ log C) is the slope of a plot surface tension vs. –log concentration curves below CMC at constant temperature.

*Minimum surface area ($A_{min}$):* The area per molecule at the interface provides information on the degree of packing and the orientation of the adsorbed surfactant molecule. The average area (in square angstrom) occupied by each molecule adsorbed on the interface[19] is given by:

$$A_{min} = \frac{10^{16}}{N\,\Gamma_{max}} \qquad 3$$

N Avogadro's number 6.023 x 1023
$\Gamma_{max}$ maximum surface excess in mole / $cm^2$

*Free energy of micellization and adsorption:* The thermodynamic parameters of adsorption and micellization of the synthesized cationic surfactants were calculated according to Gibb's adsorption equations as follows[20]:

$$\Delta G^{o}_{mic} = RT\ ln\ (CMC) \qquad 4$$

$$\Delta G^{O}_{ads} = \Delta G^{O}_{mic} - 6.023\ X10^{-1}\ X\ \pi_{CMC}\ X\ A_{min} \qquad 5$$

*Corrosion inhibition measurements*

*Weight loss*

The experiments were performed with carbon steel specimens having a composition (wt%): 0.21 C, 0.035 Si, 0.25Mn, 0.082 P, and the remainder is Fe. The carbon steel was abraded with a series of emery papers (grades 320, 500, 800 and 1200) and then washed with distilled water and acetone .After weighing accurately (using Mettler AG104 0.1 mg Analytical Balance), the specimens were immersed in 250 ml beaker contained 250 ml 1 M HCl with and without addition of different concentrations (25, 50, 100, 200, and 400 ppm by weight) of the testedinhibitorsat 25 $^{o}$C. After 24 hr, the specimens were taken out, washed, dried, and weighed accurately .The corrosion rate (Cr) and the inhibition efficiency ($\eta_{Cr}$%) were calculated using the following Eq. (6) and (7)[21]:

$$Cr = \frac{\Delta w}{st} \qquad 6$$

$$\eta_{Cr}\% = \frac{Cr_{uninh} - Cr_{inh}}{Cr_{uninh}}\ x100 \qquad 7$$

where ΔW is the average weight loss of three parallel carbon steel sheets (one specimen in each beaker), S is the total area of the steel specimen, and its immersion time, $Cr_{uninh}$ and $Cr_{inh}$ are the corrosion rates obtained in absence and presence of inhibitors, respectively. The specimens were immersed in the solutions without blocking any side, and the whole specimen area was considered in the calculation. Experiments were carried out in triplicate. The average weight loss of three parallel CS sheets was obtained.

*Potentiodynamic polarization measurements*

Potentiodynamic polarization measurements were conducted using a VoltaLab-PGZ-301 (France). A conventional cylindrical glass cell of 250 ml with three electrodes was used. A platinum sheet and saturated calomel electrode (SCE) were used as auxiliary and reference electrodes, respectively. The working electrode was cut in the form of disk (from the used carbon steel) with an area of 0.7 cm2 was embedded with epoxy except of the working surface area. Potentiodynamic polarization curves were obtained by varying the potential

automatically from -1000 mV to -200 mV with the scan rate of 2 mV. The inhibition efficiency ($\eta_P$ %) was calculated using Eq. (8) as follows [22].

$$\eta_P\% = \frac{i_0 - i}{i_0} x100 \qquad 8$$

where $i_0$and i are the corrosion current density values without and with inhibitors.

*Electrochemical impedance spectroscopy (EIS)*

EIS measurements were carried out using a Voltalab 40Potentiostat PGZ 301 attached with Voltamaster software .The measurements were carried out using AC signal(10 mV) peak to peak at the open circuit potential (OPC) in the frequency range of 100 kHz–50 mHz. The inhibition efficiencies ($\eta_{EIS}$%) of the tested inhibitors were calculated from the the charge-transfer resistances values at 25,50, 100, 200, and 400 ppm by weight using the following Eq( 9):

$$\eta_{EIS}\% = \frac{R_{ct} - Rct^{o}}{R_{ct}} x100 \qquad 9$$

where $R_{ct}$ and $R_{ct}$°are the charge-transfer resistances in the inhibited and uninhibited solutions, respectively**.**

## Results and Discussion

*Chemical structure*

The chemical structure of the prepared cationic surfactants was confirmed by elemental analysis, FTIR and $^1$HNMR spectra.

*FTIR Spectra*

The FTIR spectra of synthesized compounds (Fig.1) showed the following absorption bands at 1734 – 1738 $cm^{-1}$ for c=o ester group, 2850 $cm^{-1}$ for $CH_2$ group and 2919-2924 $cm^{-1}$ for $N^+$ group. The FTIR spectra confirmed the expected functional groups in the synthesized cationic surfactants.

*$^1$HNMR spectra*

$^1$HNMR spectra of synthesized cationic surfactants (Fig. 2) showed signals at: δ= 0.89 ppm (t, 3H, $CH_3$), 1.28 ppm (s, 2H, $CH_2$), 1.25 ppm (q, nH, $CH_2$), 3.82 ppm (t, 2H, $CH_2$), 3.87 ppm (s, 2H, $CH_2$), 3.6 ppm (s, 2H, $CH_2$), 7.25 ppm (d, 1H, CH phenyl) and 3.6 ppm (s, 3H, $CH_3$) where n = 18, 22 or 26 for compounds Ib, IIb and IIIb, respectively. The data of $^1$HNMR spectra confirmed the expected hydrogen proton distribution in the synthesized cationic surfactants. All the synthesized cationic surfactants have approximately the same values.

*Surface active properties*

The surface tension was measured for aqueous solutions of the prepared cationic surfactants with different concentrations (0.04 to 1.9X $10^{-5}$ mole/liter) at

20 $^{o}$C. And the data are represented in surface tension-concentration curves as shown in Fig. 3. It is clear that surface tension decreases by increasing concentration of the surfactant molecules as a result of hydrophobicity of the molecules which prefer to accumulate in the surface of the solution [23].

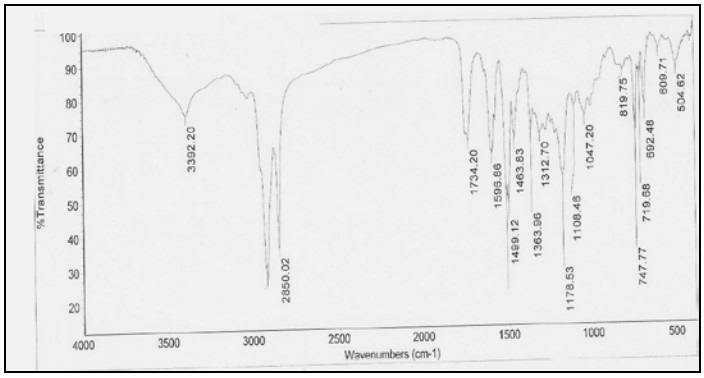


**Fig. 1 . FTIR spectra of cationic surfactant Ib.**

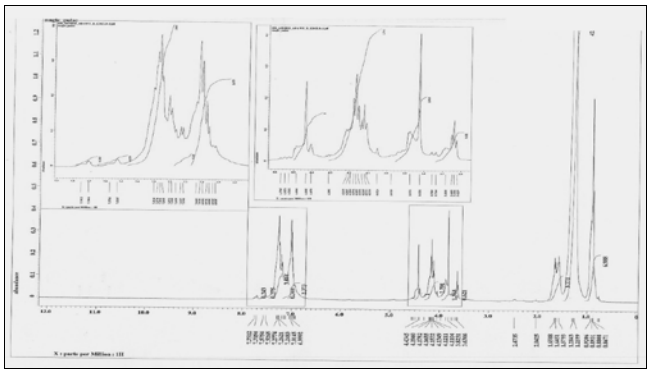

**Fig. 2 . $^{1}$HNMR spectra of cationic surfactant Ib.**

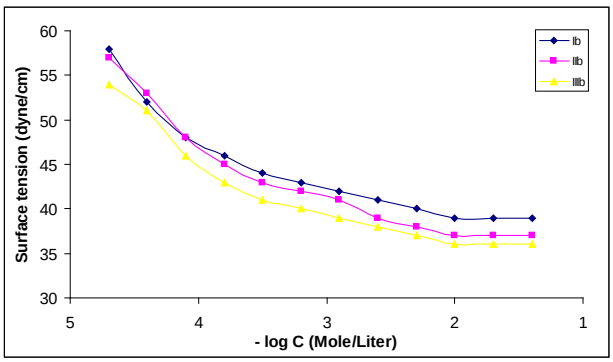


**Fig. 3. Surface tension vs. – log concentration of surfactants at (20 $^{o}$C).**

The values of the surface parameters are given in Table 1, the critical micelle concentration values of the prepared cationic surfactants were determined by plotting the surface tension ($\gamma$) of the surfactant solutions versus concentrations in mole/liter at 20$^{o}$C. The CMC values showing a decrease in the CMC with increasing the alkyl chain length[24]. By increasing the alkyl chain length the solubility decreases leading to concentration of the surfactant molecules at the surface and formation of micelles.

**TABLE 1. Surface properties of the synthesized cationic surfactants at 20 °C.**

| Surfactant | CMC X $10^{-4}$, mole/liter | $\pi_{CMC}$, mN/m | $Pc_{20}X10^{-5}$, mole/liter | $\Gamma_{max}$ X $10^{-11}$, mole/cm$^2$ | $A_{min}$, nm$^2$ |
|---|---|---|---|---|---|
| **Ib** | 7.8 | 32.97 | 7 | 5.46 | 3.04 |
| **IIb** | 6.9 | 32.84 | 2 | 6.18 | 2.68 |
| **IIIb** | 6.7 | 36.4 | 2 | 5.64 | 2.94 |

The most efficient surfactant is one that gives the greatest lowering in surface tension for a critical micelle concentration (CMC). According to the results of the effectiveness shown in Table 1, compound (IIIb) was found the most effective one at 20 °C, it gives 36.4 dyne/cm; it achieved the maximum reduction of surface tension at (CMC).

The efficiency ($Pc_{20}$) decreases as a result of increasing the alkyl chain length due to fast formation of mono layer of surfactants on the surface. In general maximum surface excess$\Gamma_{max}$ increases by increasing carbon chain length due to increase of the repulsion forces with the water phase so the surfactant molecules migrated to the interface. While the minimum surface area ($A_{min}$) decreases with an increase in the chain length of the hydrophobic part in the surfactant molecules due to the higher accumulation of these molecules at the interface and a smaller available area per molecule.

Also, the standard free energies of micellization and adsorption ($\Delta G^{o}_{mic}$,$\Delta G^{o}_{ads}$) were calculated and listed in Table 2 and showed that; these values are always negatives indicating these two processes are spontaneous; however, there is a greater increase in the negative value of $\Delta G_{ads}$ compared to those of micellization. This suggests the tendency of the molecules to be adsorbed at the interface.

**TABLE 2. Free energy of micellization and adsorption of the synthesized cationic surfactants at 20 °C.**

| Surfactant | $\Delta G^{O}_{mic}$, KJ/mole | $\Delta G^{O}_{ads}$, KJ/mole |
|---|---|---|
| **Ib** | -17.44 | -78 |
| **IIb** | -17.74 | -71 |
| **IIIb** | -17.81 | -82 |

*Weight loss measurements*

The corrosion of carbon steel in 1M HCl in the absence and presence of various concentrations (25–400ppm) by weight of Ib, IIb and IIIb, respectively was studied by weight loss experiments. The corrosion rate (*Cr*) and the percentage protection efficiency η% were calculated and summarized in Table 3. The results show that as the inhibitor concentration increases, the corrosion rate decreases and therefore the inhibition efficiency η% increases. It can be concluded that these inhibitors act through self-assembling on carbon steel surface and formation of a barrier layer between the metal and the corrosive media. Self-assembling of Ib, IIb and IIIb on carbon steel surface can be explained on the basis that adsorption of the inhibitor was mainly via the nitrogen atoms in the quaternary amine slate in addition to the availability of π electrons (by resonance structures) in the aromatic system.

**TABLE 3. Corrosion rate of carbon steel and inhibition efficiency obtained from weight loss for different concentrations of Ib, IIb, and IIIb in 1 M HCl .**

| Inhibitor | Concentration , ppm by weight | Cr,mgcm$^{-2}$h$^{-1}$ | η% |
|---|---|---|---|
| **Ib** | Blank | 4.4 | 0.0 |
| | 25ppm | 2.55 | 42.04 |
| | 50ppm | 2.19 | 66.49 |
| | 100ppm | 1.88 | 75.81 |
| | 200ppm | 1.73 | 80.07 |
| | 400ppm | 1.59 | 84.35 |
| **IIb** | 25ppm | 2.56 | 55.15 |
| | 50ppm | 2.02 | 71.34 |
| | 100ppm | 1.82 | 77.21 |
| | 200ppm | 1.68 | 81.58 |
| | 400ppm | 1.49 | 87.36 |
| **IIIb** | 25ppm | 2.11 | 68.5 |
| | 50ppm | 1.95 | 73.61 |
| | 100ppm | 1.62 | 83.51 |
| | 200ppm | 1.42 | 89.51 |
| | 400ppm | 1.35 | 92.01 |

*Adsorption isotherms*

If it is assumed that corrosion occurs only in the free sites such that the covered sites have zero corrosion rates, the degree of surface coverage θ for different concentrations of Ib, IIb and IIIb were evaluated by the weight-loss method by using the following equation(10) [24]:

$$\theta = \frac{Cr_{uninh} - Cr_{inh}}{Cr_{uninh}} \qquad 10$$

where $Cr_{uninh}$ and $Cr_{inh}$ are the corrosion rates obtained in absence and presence of inhibitors, respectively.

It can be seen that the values of surface coverage increased with increasing inhibitor concentration as a result of more inhibitor molecules adsorption on the steel surface. Now, assuming the adsorption of Ib, IIb and IIIb belonged to

monolayer adsorption and ignoring the lateral interaction between the inhibitor molecules, then the Langmuir adsorption isotherm was applied to investigate the adsorption mechanism by the following equation (11) [25]:

$$\frac{C}{\theta} = \frac{1}{k} + C \qquad 11$$

The good linear relationship between C/θ and C were drawn in Fig. 4 and the parameters are listed in Table 4 . The good linear relationship between C/θ and C with correlation coefficient equal to 1 indicates that the assumption and the deduction were correct, in other words, the adsorption of Ib, IIb and IIIb on the steel surface in 1M HCl solution is well described by the Langmuir adsorption isotherm [24, 26]. The considerable deviation of the slopes from unity shows that the isotherm cannot be strictly applied. This deviation is attributable to interaction between adsorbed species on the metal surface[27]. A modified Langmuir adsorption isotherm [28,29] could be applied to this phenomenon, which is given by the corrected:

$$\frac{C}{\theta} = \frac{n}{k} + nC \qquad 12$$

The adsorption coefficient (k) increase in order Ib < IIb < IIb (Table 4), indicating that the interactions between the adsorbed molecules and the metal surface were increased with increasing surface activity of the prepared inhibitors consequently.

**TABLE 4. Parameters of linear regression between C/θ and C.**

| Inhibitor | K $mol^{-1} \times 10^{-5}$ | Slope | Linear correlation coefficient (r) |
|---|---|---|---|
| **Ib** | 0.27 | 1.13 | 0.9990 |
| **IIb** | 0.36 | 1.10 | 0.9997 |
| **IIIb** | 0.55 | 1.05 | 0.9999 |

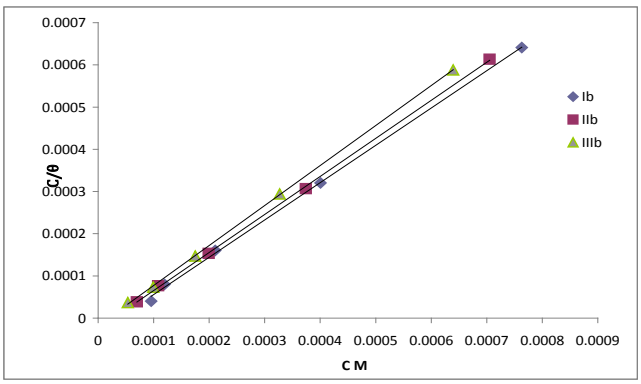


**Fig. 4. Relationship between(C/θ) and C M for carbon steel in 1 M HCl for Ib, IIb, and IIIb.**

*Electrochemical measurements*

*Potentiodynamicpolarization*

The electrochemical kinetics of metallic corrosion process can be characterized by determining the polarization parameters, such as corrosion current density ($i_{corr}$), corrosion potential ($E_{corr}$) and Tafel slopes (βa and/or βc ). The corrosion behavior can be determined by a polarization curve (log i versus E). Using Tafel extrapolation method, it is possible to obtain the corrosion current density at the corrosion potential by the extrapolation Tafel lines [30]. Thus, it was possible to determine $i_{corr}$ for all concentrations of all tested inhibitors, as well as for the blank (solution without inhibitor). The polarization curves for the carbon steel electrode in 1.0 M HCl with different inhibitor concentrations are shown in Fig. 5-7. The electrochemical parameters, namely, the corrosion potential ($E_{corr}$), corrosion current density ($i_{corr}$), anodic (βa) and cathodic (βc) Tafel slopes and inhibition efficiency (η%), are listed in Table 5 . According to the polarization curves, the presence of the inhibitors promotes a decrease in both the anodic and cathodic current densities and there is no definite trend was observed in the shift of $E_{corr}$ values in the presence of various concentrations of inhibitors, suggesting that this compound acted as mixed type inhibitor, that is, it influenced both metal dissolution and hydrogen evolution. These results indicate that the addition of the inhibitors in the corrosive solution reduces the anodic dissolution of steel and slows the cathodic evolution of hydrogen [31, 32]. Table 5 shows that the inhibition efficiency increases with increasing inhibitor concentration. This result indicates that these compounds act as adsorption inhibitors, given that more molecules are adsorbed on the metal surface as the concentration increases, promoting wider surface coverage [33].

**TABLE 5. Electrochemical parameters for carbon steel determined from polarization measurements in 1M HCl solution without and with various concentrations of Ib, IIb, IIIb.**

| Inhibitor | Dose,ppm weight | $E_{corr}$ (mV)(SCE) | $i_{corr}$(mA $cm^{-2}$) | $\beta_a$(mV $decade^{-1}$) | $B_c$(mV $decade^{-1}$) | η % |
|---|---|---|---|---|---|---|
| Ib | Blank | 622.8- | 0.1998 | 258.2 | -162.6 | 0.00 |
| | 25ppm | 568.8- | 0.1070 | 215.1 | -152.5 | 46.45 |
| | 50ppm | -613.2 | 0.0869 | 240.3 | -158.1 | 56.51 |
| | 100ppm | -625.7 | 0.0755 | 257.1 | -126.7 | 62.21 |
| | 200ppm | -594 | 0.0536 | 192.9 | -140.1 | 73.12 |
| | 400ppm | -631 | 0.0401 | 153.4 | -140.6 | 79.92 |
| IIb | 25ppm | -571.1 | 0.1053 | 216.5 | -158.7 | 47.29 |
| | 50ppm | -618.0 | 0.0804 | 267.1 | -190.1 | 59.75 |
| | 100ppm | -608.1 | 0.0527 | 183.1 | -169.1 | 73.62 |
| | 200ppm | -529.5 | 0.039 | 121.7 | -210.1 | 80.48 |
| | 400ppm | -539.3 | 0.0346 | 118.5 | -209.1 | 82.68 |
| IIIb | 25ppm | -664.9 | 0.0771 | 348.9 | -139.3 | 61.41 |
| | 50ppm | -579.5 | 0.0679 | 151.6 | -154.7 | 66.06 |
| | 100ppm | -638.9 | 0.0389 | 146.5 | -135.1 | 80.53 |
| | 200ppm | -602.4 | 0.0331 | 190.4 | -154.0 | 83.43 |
| | 400ppm | -572.1 | 0.0196 | 113.2 | -162.2 | 90.19 |

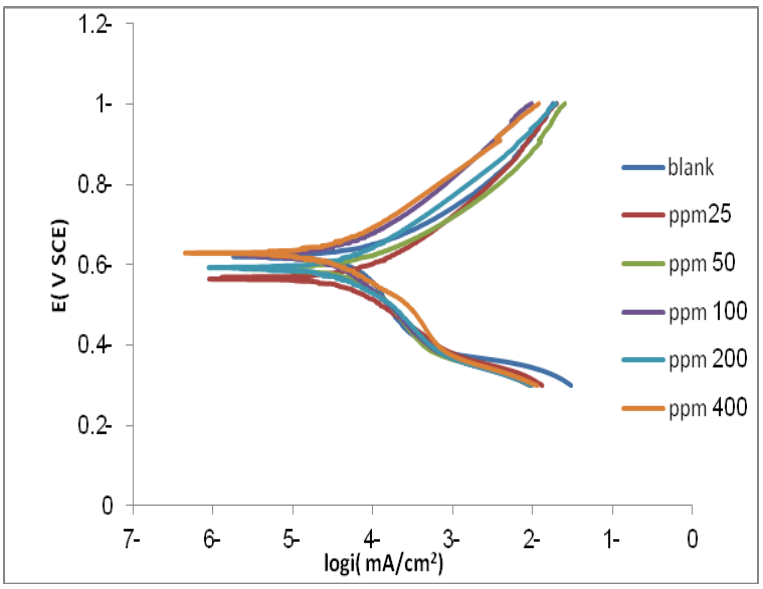


**Fig. 5. Anodic and cathodic polarization curves for carbon steel in 1M HCl at different concentrations of Ib.**

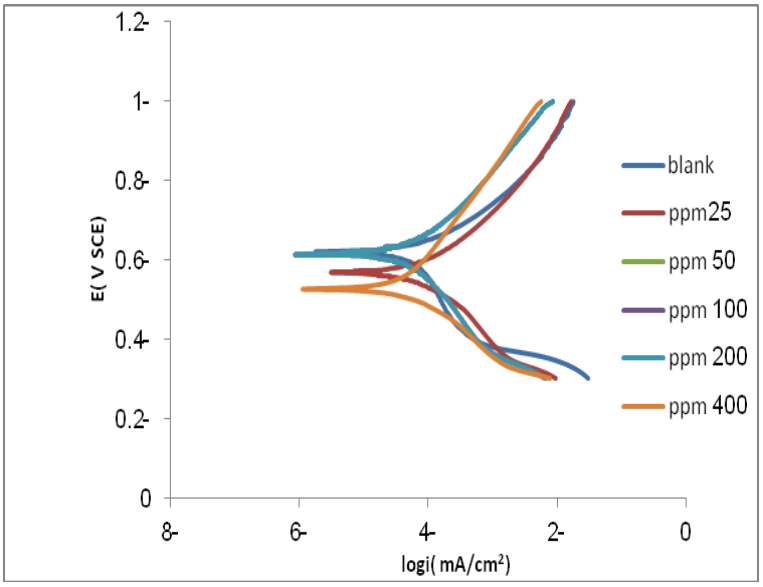


**Fig. 6. Anodic and cathodic polarization curves for carbon steel in 1M HCl at different concentrations of IIb.**

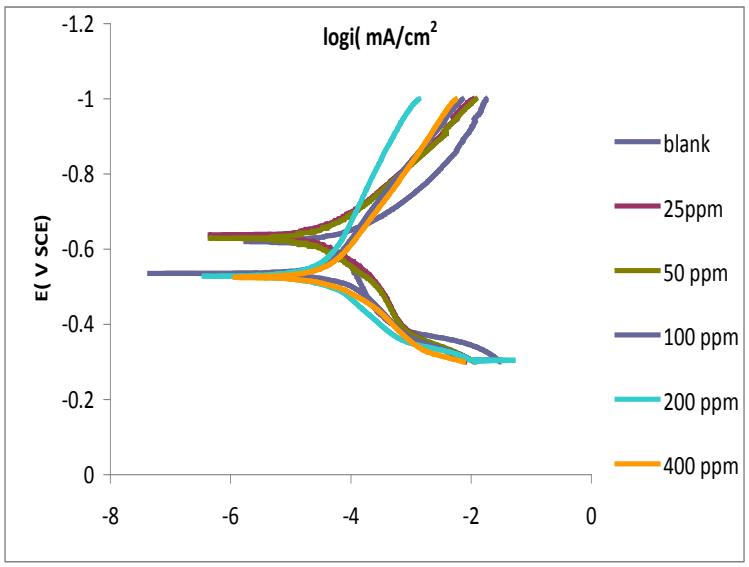


**Fig. 7. Anodic and cathodic polarization curves for carbon steel in 1M HCl at different concentrations of IIIb.**

The inhibition efficiency values in the absence and presence of different concentrations of Ib, IIb and IIIb at 25°C are comparable with those calculated from weight loss measurements, meaning that the conclusions obtained from gravimetric and electrochemical methods are in good agreement [34,35]. However, the exact values of inhibition efficiency obtained by the two measurements remain different. These differences could be attributed to the fact that the weight loss method gives average corrosion rates, while the electrochemical method gives instantaneous corrosion rates. Another possible reason may be the difference in immersion time. Similar observation has been reported by several authors [36,37].

*Electrochemical impedance spectroscopy*

The effect of inhibitor concentration on the impedance behavior of carbon steel in 1M HCl solution at 25 °C is presented in Fig. 8-10. The curves show a similar type of Nyquist plot for carbon steel in the presence of various concentrations of Ib, IIb and IIIb, respectively. As seen from Fig. 8-10, the Nyquist plots contain a depressed semi-circle, which size is increased by increasing the inhibitor concentration, indicating that the corrosion is mainly a charge transfer process [38]. The depressed semi-circle is the characteristic of solid electrodes and often refers to frequency dispersion which arises due to the roughness and other in homogeneity of the surface [39]. It is worth noting that the change in the concentration of Ib, IIb and IIIb did not alter the style of the impedance curves, suggesting a similar mechanism of inhibition suggesting

similar mechanism for the corrosion inhibition of carbon steel by synthesized inhibitors. The impedance parameters derived from these plots are given in Table 6. The double layer capacitance ($C_{dl}$) and inhibition efficiency (η%) are calculated from the following equation 12 [40]:

$$C_{dl} = \frac{1}{2\pi R_{ct} F_{apex}} \qquad 12$$

where $F_{apex}$ is the frequency at apex on Nyquist plot, and $R_{ct}$ is the charge transfer resistance value of inhibitor. As seen from the table, the $R_{ct}$ values of inhibited substrates are increased with the concentration of inhibitors. On the other hand, the values of $C_{dl}$ are decreased with increase in inhibitor concentration which is most probably due to the decrease in local dielectric constant and/or increase in thickness of the electrical double layer, suggesting that the Ib, IIb and IIIb act via adsorption at the metal/solution interface [39-41]. It could be assumed that the decrease of $C_{dl}$ values is caused by the gradual replacement of water molecules by adsorption of organic molecules on the electrode surface, which decreases the extent of the metal dissolution [39]. The inhibition efficiencies calculated from EIS (Table 6), showed the same trend as those obtained from potentiodynamic polarization plots (Table 5) and weight loss measurements (Table 4).

**TABLE 6. Electrochemical parameters of impedance for carbon steel of different concentrations of Ib, IIb, IIIb.**

| Inhibitor | Concentration,ppm by weight | $R_s\Omega cm^2$ | $R_t\Omega\ cm^2$ | $CdlμF\ cm^{-2}$ | η% |
|---|---|---|---|---|---|
| Ib | Blank | 4.7 | 122.1 | 295 | 0.0 |
| | 25ppm | 5.6 | 290.2 | 69.1 | 57.29 |
| | 50ppm | 8.8 | 558.7 | 39.87 | 78.15 |
| | 100ppm | 17.2 | 690.1 | 27.23 | 82.31 |
| | 200ppm | 1.4 | 799.6 | 22.29 | 84.73 |
| | 400ppm | 15.8 | 913.1 | 13.9 | 86.63 |
| IIb | 25ppm | 10.2 | 357 | 49.2 | 65.78 |
| | 50ppm | 14.04 | 579.4 | 34.6 | 78.92 |
| | 100ppm | 7.6 | 701.3 | 30.1 | 82.59 |
| | 200ppm | 12.7 | 943.6 | 22.7 | 87.06 |
| | 400ppm | 4.4 | 1066 | 19.4 | 88.55 |
| IIIb | 25ppm | 5.7 | 588.7 | 42.7 | 79.25 |
| | 50ppm | 6.73 | 712.6 | 31.3 | 82.86 |
| | 100ppm | 12.4 | 930.5 | 25.2 | 86.88 |
| | 200ppm | 2.8 | 1102.3 | 20.3 | 88.92 |
| | 400ppm | 0.6 | 1303 | 15.2 | 90.62 |

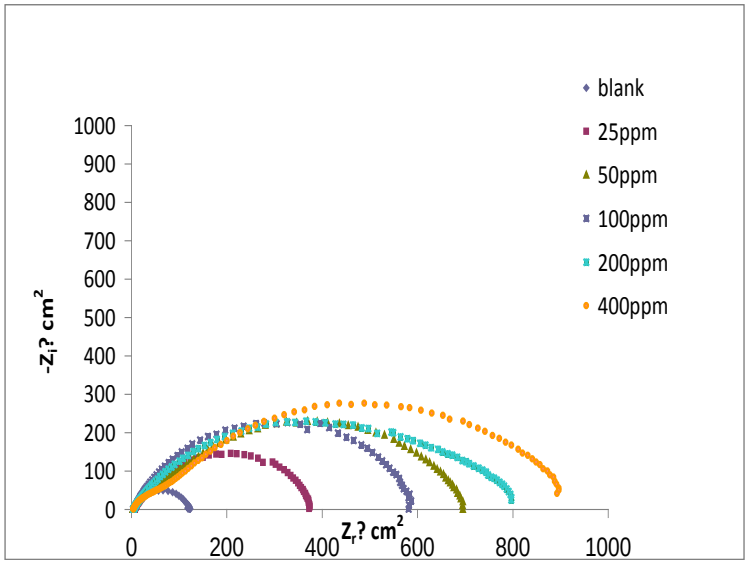


**Fig. 8. Nyquist plots for carbon steel in 1 M HCl in absence and presence of different concentrations of Ib.**

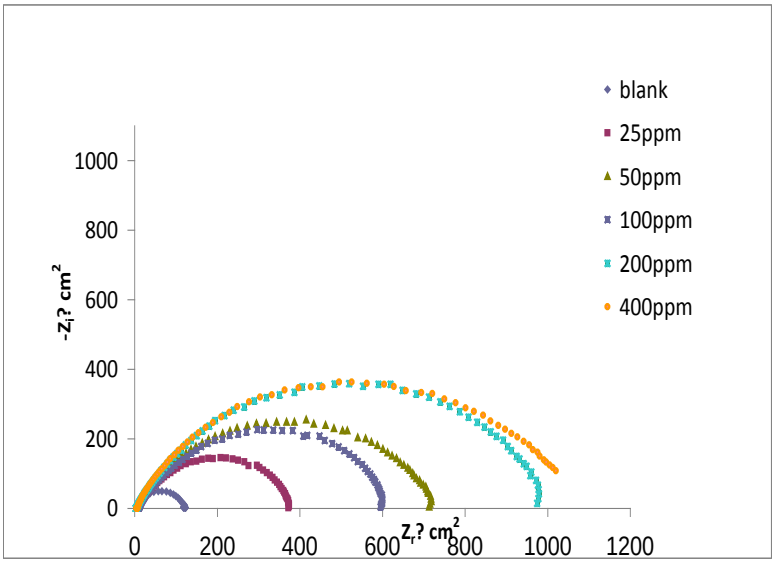


**Fig. 9. Nyquist plots for carbon steel in 1 M HCl in absence and presence of different concentrations of IIb.**

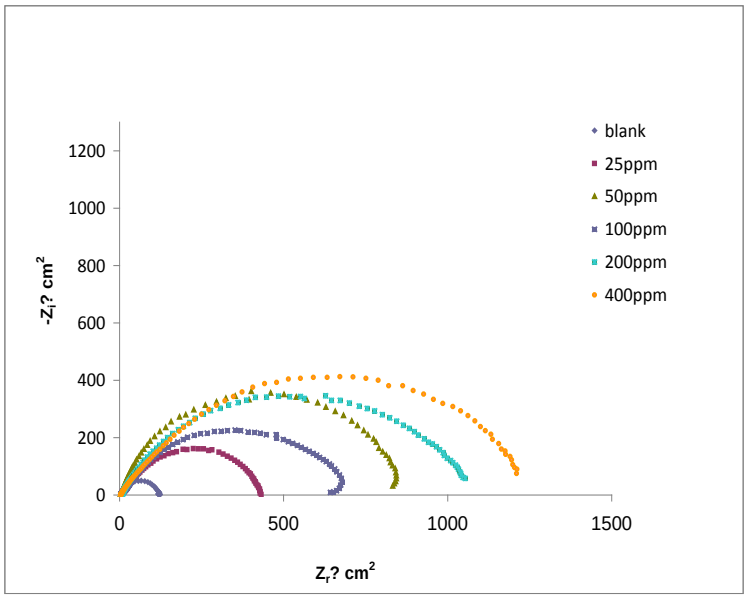


**Fig. 10. Nyquist plots for carbon steel in 1 M HCl in absence and presence of different concentrations of IIIb.**

## Conclusion

Cationic surfactants have been synthesized, and the structures were confirmed by FTIR spectra and $H^1$ NMR.

Surface parameters were measured and the thermodynamic parameters were calculated. The data showed that; the values $\Delta G_{ads,}$and $\Delta G_{mic}$ are always negatives indicating these two processes are spontaneous; however, there is a greater increase in the negative value of $\Delta G_{ads}$ compared to those of micellization. This suggests the tendency of the molecules to be adsorbed at the interface. Electrochemical studies and weight loss measurements give similar results.

Polarization measurements showed that the cationic surfactants are mixed-type inhibitors, inhibiting the corrosion of carbon steel by blocking the active sites of the metal surface.

Double-layer capacitances decrease with respect to the blank solution when these inhibitors are added. This fact may be explained on the basis of adsorption of these inhibitors on the steel surface.

**References**


1. **Fan, H.B., Fu, C.Y., Wang, H.L., Guo, X.P. and Zheng, J.S.,** *Br. Corros. J.* **37**, 122 (2002).

2. **Chetouani, A., Aouniti, A., Hammouti, B., Benchat, N., Benhadda, T. and Kertit, S.**, *Corros.Sci.* **45,** 1675–1684 (2003).

3. **Ateya, B.G., El-Andoni, B.F., El-Nizamy, F.M.A.**, *Bull. Chem. Soc. Jpn.* **54,** 3157 (1981).

4. **Migahed, M.A. and Nassar, I.F.,** *Electrochimica Acta*, **53,** 2877-2882 (2008).

5. **Rajeev, P., Surendranathan, A.O., Murthy and Ch. S.N.**, *J. Mater. Environ. Sci.* **3**, 856–869 (2012).

6. **Qiu, L., Wu, Y., Wang, Y. and Jiang, X.,** *Corros. Sci*. **50**, 576–582 (2008).

7. **Ahamad, I. and Quraishi, M.A.,** *Corros. Sci.* **51**, 2006–2013 (2009).

8. **Shukla, S.K. and Quraishi, M.A.,** *Corros.Sci.* **51**, 1990–1997 (2009).

9. **Obot, I.B., Obi-Egbedi, N.O. and Odozi, N.W.,** *Corros. Sci.* **52**, 923–926 (2010).

10. **Praveen, B.M. and Venkatesha, T.V.,** *Int. J.Electrochem. Sci.* **4**, 267–275 (2009).

11. **Asefi, D., Arami, M., Sarabi, A.A. and Mahmoodi, N.M.,** *Corros. Sci.* **51**, 1817–1821 (2009).

12. **Moura, E.F., Neto, A.O.W., Dantas, T.N.C., Junior and Gurgel, H.S.,** *Colloids Surf. A: Physicochem. Eng. Aspects*, **340**, 199–207 (2009).

13. **Branzoi, V., Branzoi, F. and Baibarac, M.**, *Mater. Chem. Phys.* **65**, 288 (2000).

14. **Atkin, R., Craig, V.S.J., Wanless, E.J. and Biggs, S.**, *Adv. Coll. Int. Sci.* **103**, 219 (2003).

15. **Reyes, Y., Rodfguez, F.J., del Rio, J.M., Corea, M. and Vazquez, F.,** *Prog. Org. Coatings*, **52,** 366 (2005).

16. **Elachouri, M., Hajji, M.S., Kertit, S., Essassi, E.M., Salem, M. and Coudert, R.,** *Corros. Sci.* **37**, 381–389 (1995).

17. **Hegazy, M.A., Badawi, A.M., Abd El Rehim, S.S. and Kamel, W.**, *Corros. Sci.* **69**, 110–122 (2012).

18. **Takeshita, T. I., Wakebe and Maeda, S.,** *J. Am. Oil Chem. Soc.* **59**, 90 (1982).

19. **Shuichi, M.**, **Kazayasu, I., Sadao, Y., Kazuo, K. and Tsuyoshi**, **Y.**, *J. Am. Oil Chem. Soc.* **67**, 996 – 100 (1991).

20. **Rosen, M. J.** "*Surfactants and Interfacial Phenomena*", Wiley, New York, **72** (1987).

21. **ASTM G1**-72, Practice for preparing, cleaning and evaluating corrosion test specimens, (1990).

22. **ASTM G3**-89, Standard practice for conventions applicable to electrochemical measurements in corrosion testing (1994).

23. **El-Sawy and Ahmed I. Adawy,** *J. Surf. Det.* **15,** 223 – 234 (2012).

24. **Ahmed I. Adawy and Mnal M. Khowdiary,** *J. Surf. Det.* **16**, 709 -715 (2013).

25. **Benabdellah, M., Touzani, R., Dafali, A., Hammouti, B. and Kadiri, S.E.,** *Mater. Lett.* **61,** 1197 (2007).

26. **Lebrini, M., Lagrenée, M., Vezin, H., Traisnel, M. and Bentiss, F.**, *Corros. Sci.* **49** 2254 (2007).

27. **Scendo, M.,** *Corros. Sci.* **49,** 373 (2007).

28. **Oguzie, E.E., Li, Y. and Wang, F.H.**, *J. Coll. Interf. Sci.* **310**, 90 (2007).

29. **Villamil, R.F.V., Corio, P., Rubin, J.C. and Agostinho, S.M.L.**, *J. Electroanal. Chem.* **535**, 75 (2002).

30. **Poorqasemi, E., Abootalebi, O., Peikari, M. and Haqdar, F.,** *Corros. Sci.* **51** 1043–1054 (2009).

31. **Emad A.Badr,** *J. Industrial and Engineering Chemistry*, **20,** 3361-3366 (2014).

32. **Lebrini, M., Lagrenée, M., Traisnel, M., Gengembre, L., Vezin, H. and Bentiss, F.,** *Appl. Surf. Sci.* **253,** 9267–9276 (2007).

33. **Safak, S., Duran, B., Yurt, A. and Turkog˘lu, G.**, *Corros. Sci.* **54,** 251–259 (2012).

34. **Bensajjay, F., Alehyen, S., El Achouri, M. and Kertit, S.**, *Anti-Corros. Methods Mater.* **50,** 402 (2003).

35. **Mu, G., Li, X. and Liu, G.,** *Corros. Sci.* **47**, 1932 (2005).

36. **El-Sherbini, Foad, E.E., Abd-El-Wahab, S.M. and Deyab, M.A.**, *Mater. Chem. Phys.* **82,** 631 (2003).

37. **Li, X., Tang, L., Li, L., Mu, G. and Liu, G.,** *Corros. Sci.* **48**, 308 (2006).

38. **Bentiss, F., Lagrenee, M., Traisnel, M. and Hornez, J.C.**, *Corros. Sci.* **41,** 789–803 (1999).

39. **Bentiss, F., Lebrini, M. and Lagrenée, M.,** *Corros. Sci.* **47,** 2915–2931 (2005).

40. **Khaled, K.F.,** *Electrochimica Acta*, **48,** 2493–2503 (2003).

41. **Behpour, M., Ghoreishi, S.M., Soltani, N., Salavati-Niasari, M. and Hamadanian, M.**, *A Gandomi,Corros. Sci.* **50**, 2172–2181 (2008).

(*Received* 30/3/2015;
*accepted* 21/4/2015)

# منـع تآكـل الصـلب الكربـونى فـى الوسـط الحمضـى باسـتخدام مـواد محضرة جديدة ذات نشاط سطحى كاتيونى

**عماد بدر و أحمد العدوى**
قسم البتروكيماويات – معهد بحوث البترول المصرى – القاهرة – مصر .

في هذه الدراسة ، تم تحضير ثلاثة مركبات كاتيونية مختلفة عن طريق تفاعل ثلاثة كحولات دهنية مختلفة مع حامض بروموا سيتك ثم مفاعلة الناتج مع ثنائى فنيل أمين ثم تكوين ملح الأمين الرباعى بالتفاعل مع ثلاثنيثيل الفوسفات تم اثبات التركيب للموادالمحضرة عن طريق FTIR,$^{1}$HNMR

تم قياس التوتر السطحى لمحاليل هذه المواد وحساب المعاملات الديناميكية الحرارية لهذه القياسات.

منع التآكل بواسطة هذه المركبات تم قياسه بثلاث طرق هى الفقد فى الوزن والاستقطاب الأنودى الكاثودى والمعاوقة الكهروكيميائية . كفاءات منع التآكل التى استنبطت من الطرق الثلاث فى تطابق جيد . كشفت منحنيات الاستقطاب الأنودى الكاثودى أن المركبات قيد الدراسة بمثابة مثبطات مختلطة.